Received: 21 July 2018 | Revised: 24 August 2018 | Accepted: 26 September 2018

DOI: 10.1002/jms.4298

RESEARCH ARTICLE

WILEY Journal of MASS SPECTROMETRY

w-Type ions formed by electron transfer dissociation of Cys-containing peptides investigated by infrared ion spectroscopy

Lisanne J. M. Kempkes[1] | **Jonathan Martens**[1] | **Giel Berden**[1] | **Jos Oomens**[1,2]

[1] Radboud University, Institute for Molecules and Materials, FELIX Laboratory, Nijmegen, The Netherlands

[2] Van't Hoff Institute for Molecular Sciences, University of Amsterdam, Amsterdam, The Netherlands

Correspondence
Jos Oomens, Radboud University, Institute for Molecules and Materials, FELIX Laboratory, Toernooiveld 7, 6525 ED Nijmegen, The Netherlands.
Email: j.oomens@science.ru.nl

Funding information
NWO; Rekentijd, Grant/Award Number: 16327; VICI, Grant/Award Number: 724.011.002

Abstract

In mass spectrometry-based peptide sequencing, electron transfer dissociation (ETD) and electron capture dissociation (ECD) have become well-established fragmentation methods complementary to collision-induced dissociation. The dominant fragmentation pathways during ETD and ECD primarily involve the formation of *c*- and $z^{\bullet}$-type ions by cleavage of the peptide backbone at the N—C_{α} bond, although neutral losses from amino acid side chains have also been observed. Residue-specific neutral side chain losses provide useful information when conducting database searching and de novo sequencing. Here, we use a combination of infrared ion spectroscopy and quantum-chemical calculations to assign the structures of two ETD-generated *w*-type fragment ions. These ions are spontaneously formed from ETD-generated $z^{\bullet}$-type fragments by neutral loss of 33 Da in peptides containing a cysteine residue. Analysis of the infrared ion spectra confirms that these $z^{\bullet}$-ions expel a thiol radical ($SH^{\bullet}$) and that a vinyl C=C group is formed at the cleavage site. $z^{\bullet}$-type fragments containing a Cys residue but not at the cleavage site do not spontaneously expel a thiol radical, but only upon additional collisional activation after ETD.

KEYWORDS

cysteine, electron transfer dissociation, IRMPD spectroscopy, peptide dissociation, *w*-type ions

1 | INTRODUCTION

Mass spectrometry data in combination with bioinformatics algorithms form a key technology for peptide and protein sequencing, including the identification of posttranslational protein modifications.[1,2] Particularly with the advent of top-down proteomics and the sequencing of post-translational protein modifications, electron induced dissociation methods—either electron capture or electron transfer dissociation (ECD or ETD)—have become popular.[3,4] The dominant ETD and ECD fragmentation pathways involve cleavage of the N-C_{α} bonds resulting in the formation of *c*- and $z^{\bullet}$-type ions[5-8] (see Scheme 1). Neutral loss fragments including those from the residue side chains are also commonly observed.[9-16] Side chain losses can confirm sequence assignments, improve database matching scores, and can be useful in de novo sequencing[14]. It is therefore useful to train sequencing algorithms to recognize neutral loss fragments in addition to sequence ions.[17] Neutral losses from residue side chains in radical ExD sequence ions have for instance been used to distinguish between leucine and isoleucine residues and to identify isomeric amino acid combinations.[17-20] On the other hand, extensive formation of nonsequence ions due to entire or partial side-chain losses, especially when remote from the backbone cleavage site, may severely complicate database searching.[21]

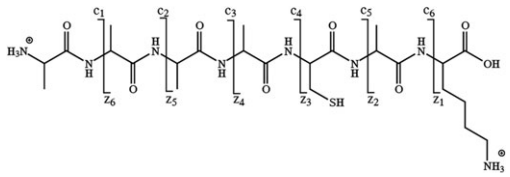

SCHEME 1 Overview of expected electron transfer dissociation sites cleaving the peptide backbone at one of the N—C_α bonds, generating N-terminal *c*-ions and/or C-terminal *z*-ions. The *z*-ions are radical species

Mechanistically, neutral loss from radical $z^\bullet$-type ions has been explained by several charge-remote fragmentation pathways.[10,21-23] Migration of the radical may occur from the original site of cleavage at the C_α atom to the C_β and C_γ positions of the same residue or to C_α, C_β, and C_γ atoms in neighboring residues.[14,18,20,21,24,25] Subsequent expulsion of a neutral radical generates even-electron fragment ions in the mass spectrum, which have been suggested to adopt a *w*-type fragment ion structure by cleavage of the C_β—C_γ bond of the N-terminal residue and the formation of a double bond between the C_α and C_β atoms (direct formation). Alternatively, cyclic *u*-type fragments may form as a result of bond formation between the N-terminal C_α atom and the C_β atom of the adjacent residue.[16,18,21,26] A possible mechanism for the loss of the entire side chain involves H-atom abstraction from the C_γ and subsequent α-cleavage and expulsion of the side chain as an even-electron neutral species, leaving the radical on the peptide backbone.[21]

Fung and Chan systematically investigated neutral loss product ions from ECD-generated $z^\bullet$-type ions using the doubly charged peptides $[RGGGXGGGR+2H]^{2+}$, where X denotes one of the 20 naturally occurring amino acid residues.[27] Residues that were shown to undergo secondary loss of a neutral radical, thus leaving behind an even-electron charged fragment, include among several others cysteine (Cys), the subject of investigation here. Even-electron neutral losses from residue side chains were also reported for various other amino acid residues.[8,24,27,28]

Cys-specific ExD pathways have been discussed in several studies.[23,27,29] For $z^\bullet$-type fragments from Cys-containing peptides, secondary fragmentation by loss of a 33-Da neutral fragment is common and is attributed to loss of a thiol radical ($SH^\bullet$). For z_6- and larger $z^\bullet$-type ions, neutral loss of CH_2S (46 Da) has also been observed.[27] ETD on $[AACAR+2H]^{2+}$ generated the z_4-ion (*m*/*z* 404) and the z_3-ion (*m*/*z* 333), where the intensity of the z_3-ion was significantly decreased by spontaneous loss of the SH radical, forming a secondary product at *m*/*z* 300.[29] ECD studies on peptides containing modified cysteine residues, such as carboxymethylated or carbamidomethylated Cys residues, report neutral losses corresponding to the modified Cys side chain.[30] The odd-electron neutral loss of $C_2H_4NOS^\bullet$ (90 Da) has also been observed in a negative electron-transfer dissociation process on a doubly negatively charged ion containing carbamidomethylated Cys residues.[31]

In related studies not actually involving ExD, the CID fragmentation behavior, and possible radical migration in open-shell cations of Cys and Cys-containing peptides have been studied by theoretical[31-33] as well as experimental methods.[16,23,35-40] In experimental studies, CID-induced loss of nitric oxide from protonated S-nitrosocysteine is an efficient way to form radical cations of Cys and Cys-containing peptides.[35,36] Hao and Gross[36] showed that CID fragmentation of Cys-containing peptide radicals yields fragmentation similar to ExD experiments. Fragmentation reactions of radical cations of Cys-containing di- and tripeptides were found to be radical-driven or charge directed, leading to losses of $SH^\bullet$ and CH_2S, respectively.[23] Analogous CID fragmentation products were found for $[GlyCysArg]^{\bullet +}$ [38]. Observed CID products of the radical cation of the Cys amino acid were $HOCO^\bullet$, CH_2S, $CH_2SH^\bullet$, and H_2S,[35] while Cys-containing peptide radicals expel $SH^\bullet$ and CH_2S.[35] Theoretical investigations suggested that loss of a $HOCO^\bullet$ radical is energetically favored for the amino acid, followed by loss of the thiol radical and loss of the side chain ($CH_2SH^\bullet$).[32-34]

Although the vinyl structure of the *w*-type fragment ion has often been assumed (see Scheme 2), experimental verification of this structure is scarce. Here, we use infrared multiple-photon dissociation (IRMPD) spectroscopy[41-48] to experimentally confirm their structure for two *z*-33 ETD fragments from Cys containing peptides. Several previous reports have made use of IR and UV photodissociation action spectroscopy methods to characterize ETD and ECD product ion structures.[41,47-57]

2 | EXPERIMENTAL AND COMPUTATIONAL METHODS

2.1 | IRMPD spectroscopy

The peptides AAAACAK and AAACAAK were purchased from BIOMATIK, Canada, and used without further purification. Doubly protonated peptide ions were generated by electrospray ionization from 10^{-7}-M solutions in 50:50 acetonitrile : water with 0.5% formic acid and mass selectively stored in a modified 3-D quadrupole ion trap mass spectrometer (Bruker, AmaZon Speed ETD).[42,48] The $z^\bullet$- and *w*-type fragment ions were produced via an ion-ion reaction with the fluoranthene radical anion for 300 ms. Ions of interest were then mass isolated in the trap, and their IRMPD spectra were measured using the free electron laser FELIX.[58,59] Ions were irradiated by two macropulses, each pulse having an energy of 10 to 60 mJ, at a repetition rate of 10 Hz and a bandwidth of ~0.5% of the center frequency. Relating parent and fragment ion intensities as the fragmentation yield (ΣI [fragment

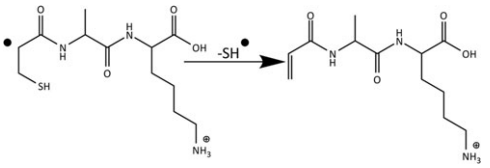

SCHEME 2 *z*-Type electron transfer dissociation fragments expected for *z*-ions with a Cys residue at the cleavage site are not observed. Instead, a *w*-type ion lower in mass by 33 Da is observed due to additional neutral loss of a thiol radical. These *w*-type ions have generally been hypothesized to possess a vinyl group at the fragment's N-terminus

ions]/ΣI [parent + fragment ions]), and plotting the yield as a function of laser frequency generates an infrared spectrum. The yield is linearly corrected for frequency-dependent variations in the laser power, and the infrared frequency is calibrated using a grating spectrometer.

2.2 | Computational chemistry

Optimized molecular geometries and theoretical infrared spectra were obtained using density functional theory (DFT) calculations as implemented in Gaussian 09 revision D01.[60] The potential energy surface was explored to locate the lowest energy minima by using a molecular mechanics/molecular dynamics approach employing AMBER 12.[61] Within AMBER an initial geometry optimization has been performed, followed by a simulated annealing procedure up to 500 K yielding 500 structures. These structures were reduced to about 20 to 30 candidate structures by considering their structural similarity setting appropriate rms criteria. In the final step, these candidate structures were optimized using DFT and their harmonic vibrational spectra were calculated. All computed harmonic vibrational frequencies were scaled by 0.975 and convoluted with a 25 cm^{-1} full width at half maximum Gaussian line shape to facilitate comparison with experimental spectra. Structure optimization, thermodynamic corrections, and frequency calculations were performed using B3LYP/6-31++G(d,p). Geometries and relative energies of conformers were verified at the M06-2X/6-31++G(d,p) level of theory. Single-point electronic energies were also obtained at the MP2(full)/6-31 + G(d,p)//B3LYP/6-31++G(d,p) level for comparison. The computational procedure is described in more detail elsewhere.[43,62,63]

3 | RESULTS AND DISCUSSION

Figure 1 shows the ETD mass spectra for the two doubly protonated heptapeptides AAAACAK and AAACAAK investigated in this study, having a Cys residue in the third and fourth position from the C-terminus, respectively. The identified ETD fragment ions are annotated in Figure 1. As a consequence of the basic Lys residue at the C-terminus, the series of $z^{\bullet}$-type fragment ions are nearly complete, except for the smallest ions.

Interestingly, for AAAACAK—with Cys in the third position from the C-terminus—the z_3 fragment is missing, but instead, a peak 33 Da lower in mass is observed. Analogously, for AAACAAK, the z_4 ion is missing and instead a peak at the nominal mass of z_4–33 is observed. We observe that neutral loss of a thiol radical ($SH^{\bullet}$) occurs only for $z^{\bullet}$-ions that contain a cysteine residue at the cleavage site; these fragments are commonly referred to as *w*-type ions. For the longer $z^{\bullet}$-ions, which do contain a Cys residue but not at the cleavage site; $SH^{\bullet}$ loss is not observed upon ETD. However, isolating one of these $z^{\bullet}$-ions and applying CID in an MS^3 experiment did result in expulsion of neutral fragments of 33 and 46 Da, the latter likely corresponding to loss of CH_2S (see Figures S1 and S2).

The $z^{\bullet}$-type ETD fragment ions that underwent neutral loss of 33 Da were investigated using IRMPD spectroscopy to determine their molecular structures. Upon IRMPD of the z_3-33 ETD fragment ion, ie, the w_3-ion, dissociation is observed into *m/z* 147 (y_1-ion), *m/z* 129 (Lys-residue), and *m/z* 84 (fragment of Lys residue). For the w_4 ETD fragment ion, IRMPD leads to fragmentation channels *m/z* 218 (y_2-ion), *m/z* 147 (y_1-ion), and *m/z* 129 (Lys-residue). IRMPD spectra are constructed including fragmentation into all of these mass channels.

The left panel of Figure 2 shows the IRMPD spectrum of the w_3 fragment ion from $[AAAACAK+2H]^{2+}$ at *m/z* 272, and that of the w_4 fragment ion from $[AAACAAK+2H]^{2+}$ at *m/z* 343 is shown in the right panel. For both these z_3-33 and the z_4-33 ions, computed spectra for a structure containing a vinyl group at the N-terminus match favorably with the experimental spectra. In this structure, the radical thiol group is expelled from the cysteine side chain and a double bond is formed

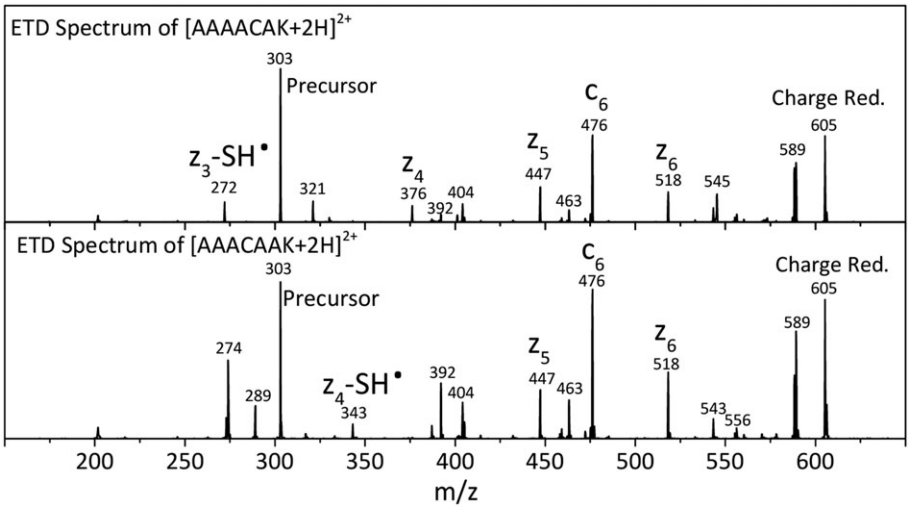

FIGURE 1 Electron transfer dissociation (ETD) mass spectra of (top) $[AAAACAK + 2H]^{2+}$ and (bottom) $[AAACAAK + 2H]^{2+}$. ETD fragment ions are annotated. Neutral loss of an $SH^{\bullet}$ radical is observed for the $z_3^{\bullet}$ fragment from AAAACAK and for the $z_4^{\bullet}$ ion from AAACAAK, ie, from $z^{\bullet}$-ions with the Cys residue at the cleavage site

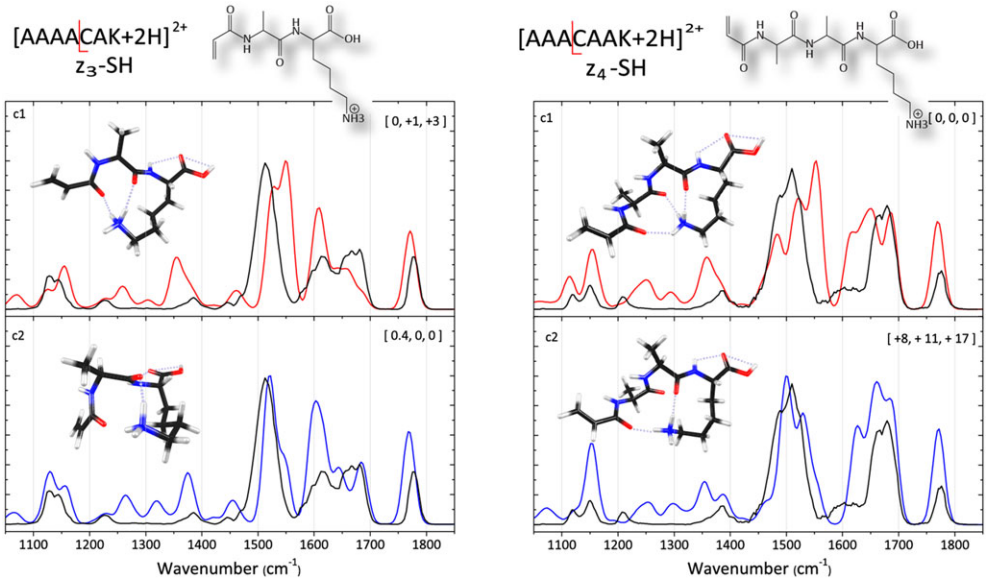

FIGURE 2 Infrared multiple-photon dissociation spectra of the (left column) z_3-33 electron transfer dissociation (ETD) fragment (w_3) from $[AAAACAK+2H]^{2+}$ at m/z 272 (black) and of the (right column) z_4-33 ETD fragment (w_4) of $[AAACAAK+2H]^{2+}$ at m/z 343 (black). The experimental spectra are compared with predicted spectra for the lowest energy structures (red) and to the qualitatively best matching calculated spectra (blue). Relative energies (kJ/mol) at the B3LYP, M06-2X, and MP2(full) levels of theory are given in the square brackets

between the C_α and C_β atoms at the site of cleavage. The calculated spectra of the lowest energy conformers (red) and the best matching conformers (blue), from a visual inspection, are presented. Computed spectra for additional conformers of these species are shown in the Figure S3.

For the w_3-ion of $[AAAACAK+2H]^{2+}$, the calculated spectra of two effectively iso-energetic conformers c1 and c2 are shown in the two panels on the left in Figure 2. Both conformers are compact structures where the protonated Lys amine group hydrogen-bonds with the two amide carbonyl oxygen atoms of the backbone. The band near 1770 cm^{-1} is attributed to the carbonyl stretch of the C-terminal carboxylic acid group. In the computed spectra of both conformers, the unresolved feature between 1600 and 1700 cm^{-1} consists of four relatively strong bands having amide C═O stretch character mixed with ammonium bending character. In addition, the band near 1660 cm^{-1} in both conformers has significant vinyl C═C stretch character mixed in. The intense feature just above 1500 cm^{-1} is due to three vibrational modes, symmetric ammonium bending and the two amide NH bending modes. The c1 calculation attributes the highest intensity to the ammonium bending mode near 1550 cm^{-1}, while the c2 calculation attributes the highest intensity to the amide NH bending modes around 1520 cm^{-1}, leading to a better match for c2. The band at 1355 cm^{-1} in c1 (mainly delocalized CH bending character) is shifted to 1375 cm^{-1} in conformer c2, the latter being in slightly better agreement with experiment.

To the right in Figure 2, two different conformers for the vinyl group containing structure of the w_4-ion from $[AAACAAK+2H]^2$ are shown along with their predicted IR spectra. The lowest-energy conformer (c1) in the top panel has its protonated Lys amine group hydrogen-bonded with all three amide oxygen atoms. The bottom panel displays a higher-energy conformer (c2) in which the ammonium group is hydrogen-bonded with just two amide oxygen atoms; the central amide moiety in the molecule is not engaged in hydrogen bonding. This leads to differences in the two predicted spectra around 1650 to 1600 cm^{-1} and 1550 to 1480 cm^{-1}. Although higher in energy at all levels of theory considered here, the c2 conformer qualitatively provides a better spectral match, and we suggest to assign this structure.

The band near 1770 cm^{-1} is again the C-terminal COOH carbonyl stretch. The feature roughly observed between 1600 and 1700 cm^{-1}, including the shoulder on the low-frequency side, is due to several normal modes mixing amide CO stretch character with asymmetric bending of the Lys NH_3^+ group. Again, the vinyl C═C stretch is mixed with the CO stretch of the adjacent amide and this mode appears at 1622 cm^{-1} in c2 and 1635 cm^{-1} in c1, at the position of the shoulder in the experimental spectrum. The c1 calculation predicts a strong, quite red-shifted CO stretch/NH_3^+ bending mode at 1613 cm^{-1}, which causes the c1 conformer to match poorly with experiment. Also the amide II experimental feature around 1500 cm^{-1} matches better with the computed spectrum of c2 than with that of c1. In both spectra, the feature comprises four intense bands, the symmetric NH_3^+ bending mode and three amide NH bending modes. The ammonium bending mode is predicted near 1550 cm^{-1} for both conformers, but is 4 times more intense in c1 than in c2, explaining the better match with experiment for c2. The remainder of the spectrum is analogous to that of the w_3-ion, with the C-terminal COH bending mode near 1150 cm^{-1} as the most prominent peak.

Secondary neutral loss from $z^\bullet$-type ions from ExD—and thiol loss from $z^\bullet$-type ions containing Cys residues in particular—leading to w-type ions has been addressed in various investigations.[14,16,18,21,31] The structure of w-type ions is commonly assumed

to involve a double bond between the α- and β-carbon atoms of the residue at the cleavage site. This fragment ion structure was hypothesized on the basis of differences in the CID MS/MS behavior of $z^{\bullet}$-ions versus (z + 1)-ions.[20] Related, the differences in bond dissociation energies for H-atom removal from the α and β carbons have been used to rationalize the CC double bond structure of the w-ion.[16,21] Computational investigations of the potential energy surface of the dissociation reaction at the DFT level also indicate the formation of a vinyl group at the N-terminus of the w-ion.[27] However, direct experimental probing of the w-ion structure has until now not been reported to our knowledge. In this contribution, IR spectroscopy of two w-type ions formed by loss of an SH-radical from a Cys residue at the cleavage site confirms the vinyl group structure suggested previously.[14,16,18,21,27,31] Indirectly, the observation of this structure also confirms the suggested charge remote fragmentation pathways suggested.[21-23,27,31]

Other $z^{\bullet}$-type ions were observed to expel a thiol radical only upon applying additional CID activation after ETD, in line with reported higher rates of formation of w-ions compared with u-ions.[18] Also in accordance with previous studies,[27,29] loss of CH_2S (46 Da) after collisional activation was only observed for $z^{\bullet}$-ions that contain a Cys residue, but not at the cleavage site. Spectroscopic probing of the structure of these fragment ions is challenging because of the more involved ETD/CID MS^n scheme required to produce them, and the inherent lower ion yields as compared with the w-type ions; such experiments are reserved for future studies.

4 | CONCLUSION

We have reported the first infrared spectra for w-type fragment ions resulting from ETD of two Cys-containing peptides. Specifically, the mass peak at m/z 272 in the ETD mass spectrum of $[AAAACAK+2H]^{2+}$ and that at m/z 343 in the ETD mass spectrum of $[AAACAAK+2H]^{2+}$, which cannot be assigned to sequence ions but are the result of neutral $SH^{\bullet}$-loss from the radical z_3 and z_4-ions of the respective peptides, have been investigated with infrared ion spectroscopy. Evaluation of experimental and predicted IR spectra confirm that these w-type fragment ions possess a structure having a C=C double bond at their N-terminus. This structure supports the mechanism proposed for the formation of w-type fragment ions in ExD, proceeding through cleavage of the C_β-S bond of the Cys residue with concomitant formation of a double bond between the C_α and C_β atoms of the w-ion. Elimination of the $SH^{\bullet}$-group is only observed for $z^{\bullet}$-ions with a cysteine residue at the cleavage site, independent of its position of cysteine in the peptide.

ACKNOWLEDGEMENTS

We gratefully acknowledge the expert technical support of the FELIX staff and the *Nederlandse Organisatie voor Wetenschappelijk Onderzoek* (NWO) for support of the FELIX Laboratory. Financial support for this project was provided by NWO Chemical Sciences under VICI grant 724.011.002. Computing resources were generously provided by NWO Physical Sciences (EW) and the SurfSARA Supercomputer Center under grant 16327.

ORCID

Jonathan Martens https://orcid.org/0000-0001-9537-4117
Giel Berden https://orcid.org/0000-0003-1500-922X
Jos Oomens http://orcid.org/0000-0002-2717-1278

REFERENCES

1. Srikanth R, Wilson J, Bridgewater JD, et al. Improved sequencing of oxidized cysteine and methionine containing peptides using electron transfer dissociation. *J Am Soc Mass Spectrom*. 2007;18(8):1499-1506.
2. Kandasamy K, Pandey A, Molina H. Evaluation of several MS/MS search algorithms for analysis of spectra derived from electron transfer dissociation experiments. *Anal Chem*. 2009;81(17):7170-7180.
3. Riley NM, Coon JJ. The role of electron transfer dissociation in modern proteomics. *Anal Chem*. 2018;90(1):40-64.
4. Coon JJ. Collisions or electrons? Protein sequence analysis in the 21st century. *Anal Chem*. 2009;81(9):3208-3215.
5. Zubarev RA, Kelleher NL, McLafferty FW. Electron capture dissociation of multiply charged protein Cations. A nonergodic process. *J Am Chem Soc*. 1998;120(13):3265-3266.
6. Zubarev RA, Haselmann KF, Budnik B, Kjeldsen F, Jensen F. Towards an understanding of the mechanism of electron-capture dissociation: a historical perspective and modern ideas. *Eur J Mass Spectrom*. 2002;8(5):337-349.
7. Syrstad EA, Turecek F. Toward a general mechanism of electron capture dissociation. *J Am Soc Mass Spectrom*. 2005;16(2):208-224.
8. Han H, Xia Y, McLuckey SA. Ion trap collisional activation of c and z* ions formed via gas-phase ion/ion electron-transfer dissociation. *J Proteome Res*. 2007;6(8):3062-3069.
9. Cooper HJ, Hudgins RR, Hakansson K, Marshall AG. Characterization of amino acid side chain losses in electron capture dissociation. *J Am Soc Mass Spectrom*. 2002;13(3):241-249.
10. Leymarie N, Costello CE, O'Connor PB. Electron capture dissociation initiates a free radical reaction cascade. *J Am Chem Soc*. 2003;125(29):8949-8958.
11. Haselmann KF, Budnik BA, Kjeldsen F. Can the (M*-X) region in electron capture dissociation provide reliable information on amino acid composition of polypeptides? *Eur J Mass Spectrom*. 2002;8(6):461-469.
12. Cooper HJ, Hakansson K, Marshall AG. The diagnostic value of amino acid side-chain losses in electron capture dissociation of polypeptides. Comment on: "Can the (M*-X) region in electron capture dissociation provide reliable information on amino acid composition of polypeptides?". *Eur J Mass Spectrom*. 2003;9(3):221-222.
13. Xia Q, Lee MV, Rose CM, et al. Characterization and diagnostic value of amino acid side chain neutral losses following electron-transfer dissociation. *J Am Soc Mass Spectrom*. 2011;22(2):255-264.
14. Savitski MM, Nielsen ML, Zubarev RA. Side-chain losses in electron capture dissociation to improve peptide identification. *Anal Chem*. 2007;79(6):2296-2302.
15. Asakawa D, Wada Y. Electron transfer dissociation mass spectrometry of peptides containing free cysteine using group XII metals as a charge carrier. *J Phys Chem B*. 2014;118(43):12318-12325.
16. Sun Q, Nelson H, Ly T, Stoltz BM, Julian RR. Side chain chemistry mediates backbone fragmentation in hydrogen deficient peptide radicals. *J Proteome Res*. 2009;8(2):958-966.
17. Falth M, Savitski MM, Nielsen ML, Kjeldsen F, Andren PE, Zubarev RA. Analytical utility of small neutral losses from reduced species in electron capture dissociation studied using SwedECD database. *Anal Chem*. 2008;80(21):8089-8094.
18. Kjeldsen F, Zubarev RA. Secondary losses via gamma-lactam formation in hot electron capture dissociation: a missing link to complete de novo sequencing of proteins? *J Am Chem Soc*. 2003;125(22):6628-6629.
19. Wee S, O'Hair RAJ, McFadyen WD. Side-chain radical losses from radical cations allows distinction of leucine and isoleucine residues in

theisomeric peptides Gly-XXX-Arg. *Rapid Commun Mass Spectrom*. 2002;16(9):884-890.

20. Johnson RS, Martin SA, Biemann K, Stults JT, Watson JT. Novel fragmentation process of peptides by collision-induced decomposition in a tandem mass spectrometer: differentiation of leucine and isoleucine. *Anal Chem*. 1987;59(21):2621-2625.
21. Li X, Lin C, Han L, Costello CE, O'Connor PB. Charge remote fragmentation in electron capture and electron transfer dissociation. *J Am Soc Mass Spectrom*. 2010;21(4):646-656.
22. Laskin J, Yang Z, Lam C, Chu IK. Charge-remote fragmentation of odd-electron peptide ions. *Anal Chem*. 2007;79(17):6607-6614.
23. Lam AKY, Ryzhov V, O'Hair RAJ. Mobile protons versus Mobile radicals: gas-phase unimolecular chemistry of radical cations of cysteine-containing peptides. *J Am Soc Mass Spectrom*. 2010;21(8):1296-1312.
24. Cooper HJ, Hudgins RR, Hakansson K, Marshall AG. Secondary fragmentation of linear peptides in electron capture dissociation. *Int J Mass Spectrom*. 2003;228(2-3):723-728.
25. Turecek F, Julian RR. Peptide radicals and cation radicals in the gas phase. *Chem Rev*. 2013;113(8):6691-6733.
26. Kjeldsen F, Haselmann KF, Budnik BA, Jensen F, Zubarev RA. Dissociative capture of hot (3-13 eV) electrons by polypeptide polycations: an efficient process accompanied by secondary fragmentation. *Chem Phys Lett*. 2002;356(3-4):201-206.
27. Fung EYM, Chan DTW. Experimental and theoretical investigations of the loss of amino acid side chains in electron capture dissociation of model peptides. *J Am Soc Mass Spectrom*. 2005;16:1223.
28. Chung TW, Turecek F. Backbone and side-chain specific dissociations of z ions from non-tryptic peptides. *J Am Chem Soc*. 2010;21:1279.
29. Nguyen HTH, Turecek F. Near-UV photodissociation of tryptic peptide cation radicals. Scope and effects of amino acid residues and radical sites. *J Am Soc Mass Spectrom*. 2017;28:133.
30. Chalkley RJ, Brinkworth CS, Burlingame AL. Side-chain fragmentation of alkylated cysteine residues in electron capture dissociation mass spectrometry. *J Am Soc Mass Spectrom*. 2006;17(9):1271-1274.
31. Rumachik NG, McAlister GC, Russel JD, Bailey DJ, Wenger CD, Coon JJ. Characterizing peptide neutral losses induced by negative electron-transfer dissociation (NETD). *J Am Soc Mass Spectrom*. 2012;23(4):718-727.
32. Simon S, Gil A, Sodupe M, Bertran J. Structure and fragmentation of glycine, alanine, serine and cysteine radical cations. A theoretical study. *J Mol Struct (THEOCHEM)*. 2005;727(1-3):191-197.
33. Gil A, Simon S, Rodriguez-Santiago L, Betran J, Sodupe M. Influence of the side chain in the structure and fragmentation of amino acids radical cations. *J Chem Theory Comput*. 2007;3(6):2210-2220.
34. Zhao J, Siu KWM, Hopkinson AC. The cysteine radical cation: structures and fragmentation pathways. *Phys Chem Chem Phys*. 2008;10(2):281-288.
35. Ryzhov V, Lam AKY, O'Hair RAJ. Gas-phase fragmentation of long-lived cysteine radical cations formed via NO loss from protonated S-nitrosocysteine. *J Am Soc Mass Spectrom*. 2009;20(6):985-995.
36. Hao G, Gross SS. Electrospray tandem mass spectrometry analysis of S- and N-nitrosopeptides: facile loss of NO and radical-induced fragmentation. *J Am Soc Mass Spectrom*. 2005;17:1725.
37. Wee S, O'Hair RAJ, McFadyen WD. Comparing the gas-phase fragmentation reactions of protonated and radical cations of the tripeptides GXR. *Int J Mass Spectrom*. 2004;234(1-3):101-122.
38. Osburn S, Steill JD, Oomens J, O'Hair RAJ, van Stipdonk M, Ryzhov V. Structure and reactivity of the cysteine methyl ester radical cation. *Chem A Eur J*. 2011;17(3):873-879.
39. Osburn S, Berden G, Oomens J, O'Hair RAJ, Ryzhov V. Structure and reactivity of the N-acetyl-cysteine radical cation and anion: does radical migration occur? *J Am Soc Mass Spectrom*. 2011;22(10):1794-1803.
40. Sinha R, Maitre P, Piccirillo S, Chiavarino B, Crestoni M, Fornarini S. Cysteine radical cation: a distonic structure probed by gas phase IR spectroscopy. *Phys Chem Chem Phys*. 2010;12(33):9794-9800.
41. Shaffer CJ, Martens J, Marek A, Oomens J, Turecek F. Photoleucine survives backbone cleavage by electron transfer dissociation. A near-UV photodissocaition and infrared multiphoton dissociation action spectroscopy study. *J Am Soc Mass Spectrom*. 2016;27(7):1176-1185.
42. Martens J, Berden G, Gebhardt CR, Oomens J. Infrared ion spectroscopy in a modified quadrupole ion trap mass spectrometer at the FELIX free electron laser laboratory. *Rev Sci Instrum*. 2016;87(10):103108.
43. Kempkes LJM, Martens J, Grzetic J, Berden G, Oomens J. Deamidation reactions of asparagine- and glutamine-containing dipeptides investigated by ion spectroscopy. *J Am Soc Mass Spectrom*. 2016;27(11):1855-1869.
44. Polfer NC, Oomens J. Reaction products in mass spectrometry elucidated with infrared spectroscopy. *Phys Chem Chem Phys*. 2007;9(29):3804-3817.
45. Correia CF, Balaj PO, Scuderi D, Maitre P, Ohanessian G. Vibrational signatures of protonated, phosphorylated amino acids in the gas phase. *J Am Chem Soc*. 2008;130(11):3359-3370.
46. Ledvina AR, Chung TW, Hui R, Coon JJ, Turecek F. Cascade dissociations of peptide cation-radicals. Part 2. Infrared mutliphoton dissociation and mechanistic studies of z-ions from pentapeptides. *J Am Soc Mass Spectrom*. 2012;23(8):1351-1363.
47. Frison G, van der Rest G, Turecek F, et al. Structure of Electron-capture dissociation fragments from charge-tagged peptides probed by tunable infrared multiple photon dissociation. *J Am Chem Soc*. 2008;130(45):14916-14917.
48. Martens J, Grzetic J, Berden G, Oomens J. Structural identification of electron transfer dissociation products in mass spectrometry using infrared ion spectroscopy. *Nat Commun*. 2016;7:11754.
49. Shaffer CJ, Marek A, Pepin R, Slovakova K, Turecek F. Combining UV photodissociation with electron transfer for peptide structure analysis. *J Mass Spectrom*. 2015;50(3):470-475.
50. Nguyen HTH, Shaffer CJ, Tureček F. Probing peptide cation-radicals by near-UV photodissociation in the gas phase. Structure elucidation of histidine radical chromophores formed by electron transfer reduction. *J Phys Chem B*. 2015;119(10):3948-3961.
51. Nguyen HTH, Shaffer CJ, Ledvina AR, Coon JJ, Tureček F. Serine effects on collision-induced dissociation and photodissociation of peptide cation radicals of the $z^{+\bullet}$-type. *Int J Mass Spectrom*. 2015;378:20-30.
52. Shaffer CJ, Pepin R, Tureček F. Combining UV photodissociation action spectroscopy with electron transfer dissociation for structure analysis of gas-phase peptide cation-radicals. *J Mass Spectrom*. 2015;50(12):1438-1442.
53. Nguyen HTH, Shaffer CJ, Pepin R, Tureček F. UV action spectroscopy of gas-phase peptide radicals. *J Phys Chem Lett*. 2015;6(23):4722-4727.
54. Viglino E, Shaffer CJ, Tureček F. UV/Vis action spectroscopy and structures of tyrosine peptide cation radicals in the gas phase. *Angew Chem Int Ed*. 2016;55(26):7469-7473.
55. Viglino E, Lai CK, Mu X, Chu IK, Tureček F. Ground and excited-electronic-state dissociations of hydrogen-rich and hydrogen-deficient tyrosine peptide cation radicals. *J Am Soc Mass Spectrom*. 2016;27(9):1454-1467.
56. Nguyen HTH, Andrikopoulos PC, Bím D, Rulíšek L, Dang A, Tureček F. Radical reactions affecting polar groups in threonine peptide ions. *J Phys Chem B*. 2017;121(27):6557-6569.
57. Imaoka N, Houferak C, Murphy MP, Nguyen HTH, Dang A, Tureček F. Spontaneous isomerization of peptide cation radicals following electron transfer dissociation revealed by UV-Vis photodissociation action spectroscopy. *J Am Soc Mass Spectrom*. 2018;29(9):1768-1780.
58. Oepts D, van der Meer AFG, van Amersfoort PW. The free-electron-laser user facilty FELIX. *Infrared Phys Technol*. 1995;36(1):297-308.

59. Oomens J, Sartakov BG, Meijer G, von Helden G. Gas-phase infrared multiple photon dissociation spectroscopy of mass-selected molecular ions. *Int J Mass Spectrom*. 2006;254(1-2):1-19.
60. Frisch MJ, Trucks GW, Schlegel HB, et al. Gaussian09, Rev. D01, 2009, Gaussian, Inc., Wallingford, CT.
61. Case DA, Darden T, Cheatham TE III, et al. *AMBER*, 12. San Francisco: University of California; 2012.
62. Kempkes LJM, Martens J, Berden G, Oomens J. Deamidation reactions of protonated asparagine and glutamine investigated by ion spectroscopy. *Rapid Commun Mass Spectrom*. 2016;30(4):483-490.
63. Martens J, Grzetic J, Berden G, Oomens J. Gas-phase conformations of small polyprolines and their fragment ions by IRMPD spectroscopy. *Int J of Mass Spectrom*. 2015;377:179-187.

SUPPORTING INFORMATION

Additional supporting information may be found online in the Supporting Information section at the end of the article.

How to cite this article: Kempkes LJM, Martens J, Berden G, Oomens J. *w*-Type ions formed by electron transfer dissociation of Cys-containing peptides investigated by infrared ion spectroscopy. *J Mass Spectrom*. 2018;53:1207-1213. https://doi.org/10.1002/jms.4298